THE JOURNAL OF PHYSICAL CHEMISTRY A

Article

pubs.acs.org/JPCA

Surface Behavior of Malonic Acid Adsorption at the Air/Water Interface

Patrick G. Blower, Eric Shamay, Loni Kringle, Stephanie T. Ota, and Geraldine L. Richmond*

Department of Chemistry, 1253 University of Oregon, Eugene, Oregon 97403-1253, United States

ABSTRACT: The presence of organic materials adsorbed to the surfaces of aerosol particles has been demonstrated to be a determining factor in relevant atmospheric processes. Malonic acid is a small, water-soluble organic acid that is common in aerosols and is surface-active. A comprehensive investigation of the adsorption of malonic acid to the air/water interface was accomplished using vibrational sum frequency spectroscopy (VSFS) and surface tension measurements as functions of concentration and pH. Malonic acid was found to be weakly solvated at the air/water interface, and its orientation as a function of concentration was explored through different VSFS polarization schemes. pH-dependent experiments revealed that the surface-active species is the fully protonated species. Computational analyses were used to obtain depth-specific geometries of malonic acid at the air/water interface that confirm and enrich the experimental results.

1. INTRODUCTION

Organic materials are ubiquitous in the atmosphere of Earth, and their presence in aerosols plays an important role in climate conditions.[1,2] Aerosols affect climate forcing directly through the scattering and absorption of radiation and indirectly through cloud formation. These aerosols often contain a large quantity of organic matter, reaching up to 90% of the total mass of some tropospheric aerosols depending on their location. Consequently, there is increasing interest in the study of how organic matter affects aerosol surface and bulk properties. Organic acids are a particularly important class of organic material found in aerosols, varying in size and complexity from low-molecular-weight formic acid to large humic-like substances (HULIS). Dicarboxylic acids represent a sizable fraction of organic matter in aerosols because they are of low molecular weight and are soluble in water. These dicarboxylic acids, with their hygroscopic and doubly ionizable acid groups, are prevalent in the atmosphere over urban, rural, remote, and marine environments.[3−12]

Dicarboxylic acids are often the dominant class of water-soluble organics in the environment, with the shorter acids (oxalic, malonic, and succinic) being the most abundant. Deliquescence,[13] phase transitions,[14] water activities,[15] and surface tension[16−19] have been investigated for binary systems containing dicarboxylic acids such as malonic acid to aid in the predictability and modeling of these binary systems as cloud condensation nuclei (CCN).[20] Although these studies have provided a better understanding of the bulk thermodynamic properties of dicarboxylic-containing aerosols vis à vis their stability for CCN, they do not address the heterogeneous reactions[21] that can take place at the surfaces of these aerosols. For example, a recent study on halogen activation on water surfaces (i.e., a heterogeneous reaction) shows how weak acids, such as malonic acid, at a water surface can actually enhance $I_2(g)$ production in the marine boundary layer when compared to that occurring at a neat water surface.[22]

It is known from surface tension measurements[16−18] that short-chain dicarboxylic acids are surface-active. However, unlike traditional ionic alkyl surfactant molecules that have well-defined hydrophobic and hydrophilic parts, low-molecular-weight dicarboxylic acids have two hydrophilic ends (carboxylic acid moieties) connected by a hydrophobic spacer, $(CH_2)_n$. Given the prevalence of dicarboxylic acids in aerosols, surprisingly few molecular-level investigations of the behavior of dicarboxylic acids at aqueous surfaces have been conducted.

One of the more important dicarboxylic acids in the atmosphere is malonic acid (Figure 1), the focus of this study. Malonic acid, with its two carboxylic acid groups separated by a CH_2 spacer, is found in significant concentrations in aqueous environments (aerosols, freshwater, seawater, snowpack, and other forms of wet deposition).[23−26] To develop a robust molecular picture of the behavior of malonic

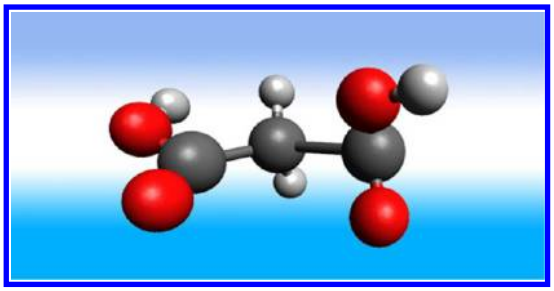

Figure 1. Schematic of malonic acid.

Received: November 2, 2012
Revised: January 11, 2013
Published: February 5, 2013

acid at a water surface, a combination of experimental and computational methods were employed in this work. The experimental approach involved surface tension measurements to provide quantitative thermodynamic data on the adsorption process and vibrational sum frequency spectroscopy (VSFS) as a means for obtaining a more microscopic picture.

VSFS is a surface-specific spectroscopy that is excellently suited for exploring the surface properties of aqueous organic systems. As a second-order nonlinear vibrational spectroscopic method, VSFS is surface-specific and can impart valuable information about the structure and orientation of an adsorbate, as well as the alteration of surface water molecules due to the presence of the adsorbate. Such experimental studies can provide valuable insights into the surface speciation and relative orientation of malonic acid at the surface and how these properties are affected as the pH of the aqueous phase changes, which can impact the charged nature of these small surfactants.

To complete the picture, molecular dynamics (MD) simulations are reported that validate the experimentally derived conclusions, assist in spectroscopic interpretations, and expand the molecular picture in dimensions not possible with the experiments. MD studies were used to directly assess the specific orientations and geometries of malonic acid on a water surface and also to examine the intermolecular interactions between neighboring water molecules. Orientational analyses of MD trajectories were used to study the geometry and orientation of malonic acid throughout a water interface. The combined results from these studies illustrate the surface density and geometry of the unique orientation that malonic acid adopts at an air/water interface, as well as the effect of the presence of multiple hydrophilic pH-dependent moieties on surface adsorption. These results provide the necessary basis to interpret ternary aqueous/organic/inorganic systems that more closely resemble aerosols in the atmosphere.

2. EXPERIMENTAL SECTION

2.1. Surface Spectroscopy. The surface specificity of VSFS makes it an excellent tool for exploring aqueous interfaces because, under the dipole approximation, the nonlinear processes that it probes are forbidden in centrosymmetric media such as bulk water. VSFS has grown in the past decade to be a highly versatile method for studying a variety of processes at water surfaces.[27−29] A brief description is provided in this section as it pertains to the experiments conducted in this study.

The VSFS experiments performed in this work involved an 800-nm beam of light overlapped in time and space with a variable-frequency beam (in the IR range) at the surface of the aqueous solution. The intensity of the resulting sum frequency signal is proportional to the square of the second-order susceptibility, $\chi^{(2)}$, which has both a resonant and nonresonant component

$$\chi^{(2)} = \chi^{(2)}_{\mathrm{NR}} + \sum_i \chi^{(2)}_{\mathrm{R},i} \tag{1}$$

Both the resonant susceptibility, $\chi^{(2)}_{\mathrm{R}}$, and the nonresonant susceptibility are proportional to the number of molecules contributing to the sum frequency response, N, and the orientationally averaged molecular susceptibility, $\langle\beta\rangle$

$$\chi^{(2)}_{\mathrm{R}} = \frac{N}{e_0}\langle\beta\rangle \tag{2}$$

Because resonant modes can overlap with one another as well as with the nonresonant background, spectral fitting is necessary to deconvolve individual peaks. A fitting procedure[30] was employed that accounts for the homogeneous and inhomogeneous line widths of vibrationally VSFS-active modes

$$\chi^{(2)} = \chi^{(2)}_{\mathrm{NR}} e^{i\psi} + \sum_\nu \int_{-\infty}^{\infty} \frac{A_\nu e^{i\phi_\nu} e^{-(\omega_{\mathrm{L}}-\omega_\nu/\Gamma_\nu^2)^2}}{\omega_{\mathrm{L}} - \omega_{\mathrm{IR}} + i\Gamma_{\mathrm{L}}} d\omega_{\mathrm{L}} \tag{3}$$

The first term in eq 3 is the nonresonant susceptibility (containing an amplitude and phase). The second term is the sum over all VSFS-active resonant modes. The resonant susceptibility is a convolution of the homogeneous (Lorentzian) line widths of the individual molecular transitions (Γ_{L}) with inhomogeneous broadening (Γ_ν). For a VSFS mode to be active, both a Raman transition and an IR dipole change must occur. This is modeled as the transition strength A_ν and is proportional to the orientationally averaged IR and Raman transition probabilities. The frequencies of the Lorentzian, resonant, and IR modes are ω_{L}, ω_ν, and ω_{IR}, respectively. Each resonant mode also has a phase value, ϕ_ν.

Selection of specific incoming and outgoing polarizations allows information about molecular orientation to be derived. This arises from the fact that, of the 27 elements of $\chi^{(2)}$, only four are simultaneously nonzero and unique (χ_{zzz}, χ_{xxz}, χ_{xzx}, and χ_{zxx}). These unique elements can be probed using incoming polarized visible and IR light and outgoing polarized sum frequency light. The polarization schemes are denoted as S (perpendicular to the plane of incidence) or P (parallel to the plane of incidence) and are given in the order of sum frequency, visible, and IR polarizations. If the incoming polarizations are selected to be S-polarized (visible) and P-polarized (IR) while the output is S polarized (SSP), the VSF response allows one to probe dipole components that are perpendicular to the plane of the interface, whereas the SPS polarization combination probes dipole components that are parallel to the plane of the interface.

Two different laser systems were used in these VSF studies. The first was used to collect data in the mid-IR region, probing the carboxylic C═O modes. This system was upgraded from a version that has been described elsewhere.[31,32] Briefly, a continuous-wave Nd:YVO4 laser (Millennia 5sJ, Spectra Physics) was used to pump a Ti:sapphire oscillator (Tsunami, Spectra Physics) that was tuned to produce ∼100-fs pulses centered at 800 nm. These pulses were then amplified using a regenerative amplifier (Spitfire Pro XP, Spectra Physics) to produce nominally 3 W of 800-nm light with a bandwidth of ∼12 nm. The output beam was split, with ∼1 W going to a home-built slicer that temporally broadened the pulse to ∼2 ps and ∼1 W going to an optical parametric amplifier (OPA-800C, Spectra Physics) for difference frequency generation (DFG) mixing and subsequent IR generation. Both the IR and visible pulses were then propagated to the air/water interface in a copropagating geometry at 45° and 60° from the surface normal, where they were overlapped in time and space to produce sum frequency pulses. The resulting sum frequency pulses were filtered by an edge filter, collected by a lens, and focused into a spectrograph that dispersed the signal onto a liquid-nitrogen-cooled charge-coupled device (CCD). All spectra were normalized to the nonresonant response of a bare gold surface and calibrated using a polystyrene standard and absorption lines from ambient water vapor. All measurements were performed at 20 °C.

The second system used to investigate the water/CH region was one that has been used extensively in previous studies in this laboratory. With this picosecond system,[33−36] sum frequency light is generated by overlapping 800-nm (~2.6 ps, 1-kHz repetition rate) and tunable (2700−4000 cm^{-1}) infrared light in a copropagating geometry at 56° and 67° from the surface normal, respectively. After filtering any reflected 800-nm light, the resultant sum frequency light is collected with a thermoelectrically cooled CCD camera in 3 cm^{-1} increments over the tunable range.

2.2. Surface Tension. Surface tension measurements were performed using the Wilhelmy plate method.[37] A force balance (KSV Instruments) was used to measure the surface tension. The solutions were placed in a clean glass dish, and great care was taken to ensure that the plate was oriented correctly with respect to the interface. The samples were allowed to equilibrate before the measurement was taken. The Pt plate was cleaned by being flamed until glowing orange and rinsed repeatedly in >18 MΩ water between measurements.

2.3. Chemicals. Malonic acid was purchased from Sigma-Aldrich (ReagentPlus 99%). NaOH was purchased from Mallinckrodt Chemicals (AR). All solutions were prepared fresh with >18 MΩ·cm water and used within 72 h. All glassware was cleaned with concentrated H_2SO_4 and NOCHROMIX and thoroughly rinsed with >18 MΩ·cm water. pH-adjusted solutions were calculated with a pH calculator[38] and then checked with litmus paper.

2.4. Computational Methods. Classical molecular dynamics (MD) simulations were performed using the Amber 11 suite of simulation programs.[39,40] A single system of water and malonic acid was initialized for simulation by creating a cubic unit cell with side lengths of 30 Å. The unit cell was then randomly packed with 900 water molecules and 17 malonic acid molecules using the PACKMOL program created to simplify construction of MD starting configurations.[41] This resulted in a malonic acid concentration of 1 M, purposefully set to be similar to that of the VSFS experimental conditions.

The initial system was energy minimized by a combination of steepest-descent and conjugate-gradient methods to reach a geometry optimization. The z axis of the system was then expanded to 100 Å, creating a large vacuum region adjacent to the aqueous cube. Periodic boundary conditions were then employed resulting in an infinite slab configuration with two aqueous/vacuum interfaces. This configuration was then evolved through MD simulation for 500 ps to equilibrate the system. The system was then evolved for 50 ns of data collection, with atomic coordinates recorded every 100 fs for a total of 500000 data points.

The simulations were performed using a time step of 1 fs. Fully polarizable models were used for both the water and malonic acid molecules. Water was simulated using the POL3 model,[42] and the malonic acid molecules were constructed using a fully atomistic model based on the Amber FF02EP force field.[43] The parameters used in the force field are listed in Table 1. The system temperature was set at 298 K, and Langevin dynamics was used to propagate dynamics through a leapfrog integrator. The particle mesh Ewald technique was used for calculating long-range electrostatic interactions with a force cutoff set to 10 Å. Water molecules were held rigid by means of the SHAKE algorithm to increase computational throughput and speed of data collection.

In all following analyses, the results obtained for molecular orientation are averaged between both of the water slab surfaces. The distance to each aqueous surface was determined for every malonic acid molecule at each time step using the method developed in a recent computational study to determine water surface locations.[44] The closer surface was always used to analyze acid orientation, and the reference axis was always set to point from the aqueous bulk outward toward the vacuum phase, normal to the plane of the water surface.

Table 1. Parameters from the AMBER FF02EP Force Field for Malonic Acid

atom	r (Å)	σ (kcal/mol)	pol (Å^3)
H_{OH}	0.2000	0.0200	0.135
H_C	1.4870	0.0157	0.135
O_H	1.7210	0.2104	0.465
$O_{C=O}$	1.6612	0.2100	0.434
C_H	1.9080	0.1094	0.878
C_{OOH}	1.9080	0.0860	0.616

3. RESULTS AND DISCUSSION

3.1. Spectroscopic Studies of Aqueous Malonic Acid.

3.1.1. Carboxylic Acid Modes. Spectroscopically probing the adsorption of malonic acid at the water surface involves two different spectral regions. The first region corresponds to the carboxylic C═O stretching modes in the 1600−1800 cm^{-1} range, and the second region in the 2700−3800 cm^{-1} range captures the CH and OH stretching modes of malonic acid and the OH stretching modes of surface water molecules. The SSP polarization combination was used in the C—H/O—H region, and both the SSP and SPS schemes were used in the C═O spectral region to measure the modes with dipole moments perpendicular and parallel to the interface, respectively.

Shown in Figure 2a are the SSP spectra along with the fitted curves of aqueous malonic acid at four concentrations. The intensity of the signal from the carboxylic C═O modes in the SSP polarization scheme increased with bulk malonic acid concentration. The intensity exhibited a progressive increase from the lowest concentration at 100 mM to 3 M, the highest concentration investigated here. In VSFS studies, intensity arises from the number density at the surface, as well as a net orientation of the molecules probed. The polarization combinations used selectively probed the direction of net orientation. Malonic acid was clearly present at the water surface with increasing population as the bulk solution concentration increased. The signal observed under SSP polarization further indicates that there was a net orientation of the dipole moment of one or both carboxylic acid groups on the diacid perpendicular to the surface plane. According to the global fits of the spectra, one peak was centrally located at 1740 ± 2 cm^{-1} with a Gaussian width of 28 ± 1 cm^{-1}. No shift in the frequency in the VSFS signal was observed with increasing bulk solution concentration.

The carboxylic C═O modes were also probed in the SPS polarization scheme, as shown in Figure 2b. The signal intensity in the SPS scheme was less than that in the SSP scheme. It should be noted that, because of the angles used for these VSFS experiments (and hence the corresponding Fresnel factors), the signal intensities for the SSP and SPS schemes were comparable. This might not always be the case for VSFS experiments because of the dependence on the local field as a function of the input angles of the visible and IR beams. As stated earlier, the SPS scheme interrogates modes that are in the plane of the interface. Because there is rotational

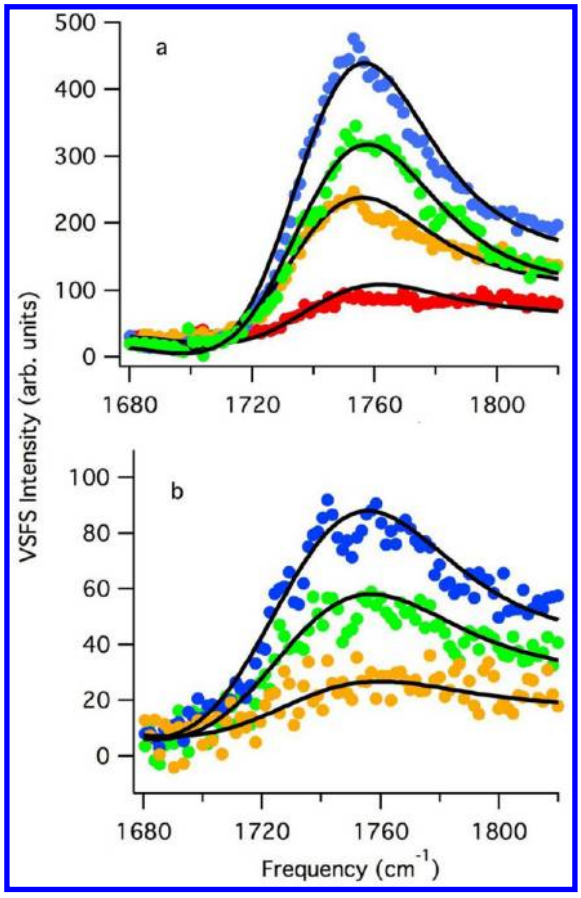

Figure 2. VSFS spectra of the carboxylic C═O mode of aqueous malonic acid (a) for SSP at concentrations of 0.1, 0.5, 1, and 3 M and (b) for SPS at concentrations of 0.5, 1, and 3 M. Fits are shown in black. The intensity of the C═O signal increased monotonically as the concentration increased.

degeneracy for modes in the plane of the interface, signal intensity can appear weaker as a result of partial canceling of the VSFS signal. As was seen with the SSP polarization scheme, the signal intensity increased as the bulk concentration of malonic acid increased. However, the fits to the spectra revealed a peak centrally located at 1730 ± 1 cm^{-1} (versus 1740 cm^{-1} for SSP polarization) with a slightly larger Gaussian width of 37 ± 1 cm^{-1} (versus 28 cm^{-1} for SSP polarization). This C═O frequency is closer to bulk aqueous values. The larger Gaussian width is consistent with a more heterogeneous environment, which supports the assertion that the SPS-active carboxylic C═O modes are in a slightly different environment than their SSP-active counterparts.

Infrared studies of malonic acid in bulk aqueous solution have shown that the carboxylic C═O modes appear at 1719 cm^{-1} for the fully protonated (H_2A) form and at 1713 cm^{-1} for the singly protonated (HA^-) form.[45] In addition, this mode is also sensitive to the degree of water solvation, with monomers in the vapor phase measured as high as 1760 cm^{-1}.[46] Surface IR studies[47,48] have shown that distinct regimes of hydrogen bonding exist for long-chain fatty acid monolayers adsorbed to the air/water interface. The regions of ∼1735−1739, ∼1715−1720, and 1700−1704 cm^{-1} are assigned as having non-H-bonded, singly H-bonded, and doubly H-bonded character, respectively. Although long-chain fatty acids and malonic acid will have different solvation properties, the trends will be similar for both. Therefore, because surface-adsorbed malonic acid has values in the range of ∼1730−1740 cm^{-1}, this indicates weak hydrogen bonding with surrounding water molecules to the carbonyl moiety.

Spectroscopic studies have shown frequencies of the carboxylic C═O mode of malonic acid up to 1740 cm^{-1}, but the studies involved either crystalline malonic acid[49] or deliquesced samples.[50] It has been established that, for such samples, the splitting of the carboxylic C═O mode is due to intermolecular hydrogen bonding (cyclic dimerization). There is a subsequent splitting of the C═O spectral features into an out-of-phase mode that is IR-active at higher wavenumbers (∼1740 cm^{-1}) and an in-phase Raman-active mode at lower wavenumbers (∼1685 cm^{-1}).[49] In our raw spectra (before normalization), there was evidence of a very weak signal appearing around 1690 cm^{-1}, which was seen only in the SSP spectra. Although this signal might be evidence of dimerization, the extremely weak signal makes any analysis very difficult, so no analysis was pursued here. In addition, if symmetric cyclic were dimers being formed, the signal would disappear because the inversion center would be sum-frequency-inactive.[51] It should be noted that all VSFS spectra recorded in this study consisted of relatively weak signals; consequently, the normally negligible nonresonant background interfered with the signal on the blue side of the spectra, so that the VSFS signal did not return to zero on the blue side of the spectra. This interference has been seen before in VSFS studies of carboxylic C═O modes[52] and nitrate modes[32] at aqueous interfaces.

Based on the SSP and SPS spectra, it is evident that C═O oscillators from malonic acid have frequencies that are blue-shifted with respect to those of both bulk dicarboxylic acid and surface carboxylic acid (e.g., hexanoic acid).[31] This is consistent with weak hydrogen bonding of the C═O mode to water. In addition, the responses from SSP and SPS polarizations are not equivalent, implying that these experiments are sampling two different hydrogen-bonding environments. These results indicate that the adsorption of malonic acid is more complex than simple alkyl carboxylate surfactant adsorption and requires further exploration to fully understand its adsorption on a water surface.

3.1.2. CH and OH Spectral Regions. In addition to probing the carboxylic C═O modes of malonic acid, we investigated the spectral region associated with the CH modes of malonic acid (∼2900 cm^{-1})[28] to develop a more comprehensive picture of the adsorbate structure. Also investigated were the OH stretching modes of water as a means of determining how the presence of the adsorbate alters the surface water structure and bonding in three spectral regions. A simple picture that has evolved from many VSFS studies of water is that the free-OH region (∼3700 cm^{-1}) corresponds to the response of water OH oscillators that have minimal interaction with nearby water molecules and, in fact, are vibrationally decoupled from the hydrogen-bonding network of bulk water. These modes are most affected by adsorbates at the topmost layer of the interface (nearest the vapor phase). At much lower frequencies reside the OH oscillators corresponding to the most highly coordinated surface water molecules (∼3200 cm^{-1}). These water molecules lie deeper in the interfacial region and are consequently more sensitive to the presence of interfacial ions. Oscillators residing in the region corresponding to intermediate degrees of hydrogen bonding and interfacial depths are located between these two regions (∼3400 cm^{-1}).[53−58]

Figure 3 shows six SSP spectra of the water/CH region for three different concentrations of malonic acid, along with the

dx.doi.org/10.1021/jp310851j | J. Phys. Chem. A 2013, 117, 2529−2542

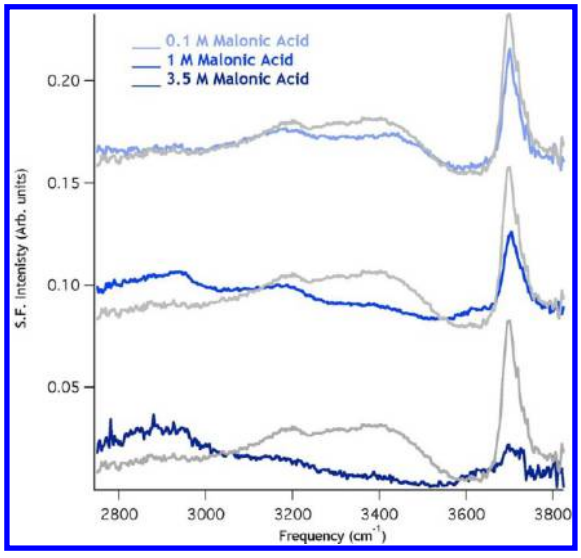

Figure 3. VSFS of water/CH region for 0.1, 1, and 3.5 M aqueous malonic acid. The gray spectra are of neat water.

spectrum of neat water in gray for comparison. Considering first the CH stretching region (2800−3000 cm^{-1}), as the malonic acid solution concentration increased, there was a corresponding increase in intensity in this region. Unfortunately, the overlap between the OH modes and the CH modes makes distinct spectral characterization difficult in this region. Nevertheless, the broad region between 2800 and 3000 cm^{-1} is attributed to the carboxylic OH stretching of malonic acid. This attribution is based on isotopic VSFS studies of selectively deuterated succinic acid, $(COOH)_2(CD_2)_2$, in D_2O and H_2O.[59] This carboxylic OH stretch is attributed to hydrogen-bonding interactions between the OH and water[60] and is consistent with IR studies of aqueous dicarboxylic acids.[61]

The overall trend observed is that, with increasing malonic acid concentration, there was a corresponding increase in signal in the CH region. A sharp peak appearing at 2945 cm^{-1} was assigned to the CH_2 stretching mode for succinic acid at the air/water interface for VSFS experiments in both SSP and SPS polarization schemes.[59] However, there was no evidence of a sharp peak indicative of CH_2 modes at the surface even at the highest concentration. The increase in this region thus most likely reflects the hydrogen bonding of the OH of the dicarboxylic acid. It is concluded that the absence of any observation of CH_2 modes is due to an orientational averaging effect. This hypothesis is addressed further in section 4.

Considering next the region corresponding to the response of water OH modes, upon adsorption of malonic acid, a corresponding decrease in the free-OH signal occurred with increasing malonic acid in bulk solution. This decrease was also observed in the 3400 cm^{-1} region corresponding to somewhat stronger but still relatively weakly bonded surface water molecules. A new peak formed above 3600 cm^{-1} that increased in intensity as the bulk concentration increased. This peak has been attributed to solvation of ions[62] and would result from the presence of hydronium ions, H_3O^+. Interestingly, the free-OH signal did not fully disappear even at concentrations of 3.5 M, indicating that the water surface was not completely covered by malonic acid. This is unlike alkyl nonionic surfactants [e.g., long-chain alcohols, sugar surfactants, alkyl poly(ethylene oxide) surfactants], for which the free-OH signal is virtually absent once complete surface coverage is reached.[63] These results then suggest that malonic acid adsorption does not completely disrupt water at the topmost layer and that malonic acid must not pack tightly enough to fully cover the surface. This issue will be addressed further in the next section. The spectral characteristics of water at longer wavelengths are consistent with an increased presence of malonic acid at the surface. The increase in the OH response around 3200 cm^{-1} is consistent with progressively stronger surface OH bonding with increased concentration of malonic acid. However, as noted earlier, the signals from overlapping modes complicate further interpretation in this region.

3.2. Surface Tension of Malonic Acid and Comparison to VSFS. Surface tension, as a macroscopic property, reflects the overall surface concentration, whereas VSFS simultaneously measures both surface concentration (number density at the surface) and molecular orientation.[51] By combining the results of these two complementary techniques, the surface density and orientation can be decoupled. This allows for a more complete picture of the adsorption of malonic acid than can be obtained from either technique alone.

The surface tension of malonic acid on H_2O was investigated[16,19] in previous studies. The surface pressure results obtained here are in excellent agreement with these

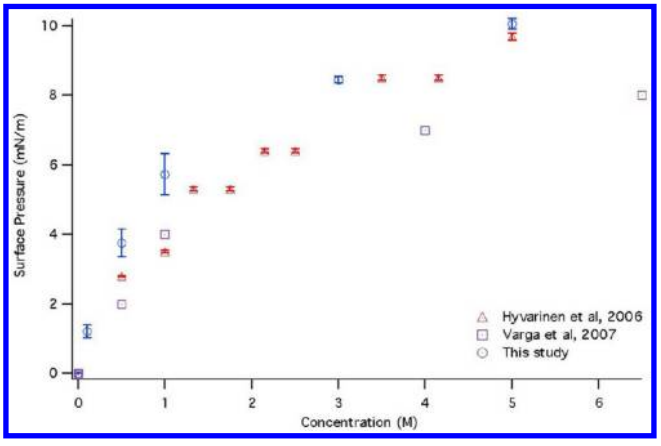

Figure 4. Plot of malonic acid concentration versus surface pressure. Shown are data from refs 16 and 19 and this study.

earlier works and are plotted in Figure 4. The Gibbs adsorption equation was employed[64]

$$\Gamma_i = -\frac{1}{RT}\left(\frac{\delta\pi}{\delta \ln a_i}\right)_T \quad (4)$$

where Γ_i is the maximum (limiting) surface excess, π is the surface pressure in mN/m, and a_i is the activity. By plotting the surface pressure versus the natural logarithm of the activity, the maximum surface excess can be calculated. Activity coefficients were obtained from Clegg and Seinfeld.[65] The area per molecule can then be obtained through[64]

$$a_1^s = 10^{23}/N\Gamma_i \quad (5)$$

where N is Avogadro's number. The value of a_1^s calculated from these data is 191 $Å^2$/molecule. This comparatively large molecular area corroborates the VSFS data from the water region, where the free-OH signal did not disappear at high concentrations (3.5 M), and confirms that malonic acid does not pack tightly at the air/water interface.

dx.doi.org/10.1021/jp310851j | J. Phys. Chem. A 2013, 117, 2529−2542

Figure 5 shows a comparison between the trends in the surface pressure data and the changes in the VSFS amplitude of

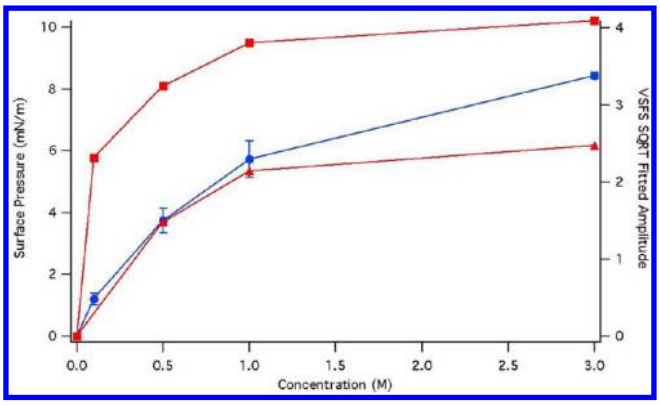

Figure 5. Plot of surface pressure versus square root of the fitted VSFS amplitude for SSP and SPS C═O modes.

the C═O mode (SSP and SPS) with malonic acid concentration. As the bulk concentration of malonic acid increased from 0 to 3 M, the surface pressure increased; further increases in concentration did not affect the surface pressure substantially, and at higher concentrations, the measurement was limited because the solubility limit of malonic acid in water was eventually reached.[16] There was an analogous rise in the square root of the VSFS intensity (the concentration dependence of the sum frequency field is the square root of the intensity)[66] of the VSFS C═O (SSP and SPS) signal over the same concentration range. This indicates that the adsorption of malonic acid to the air/water interface does not change orientation as a function of concentration. To confirm this behavior, the surface coverage as a function of concentration was calculated. To determine the surface concentration at any bulk concentration, the Frumkin equation was employed[64]

$$\pi_2 = -RT\Gamma_i \ln(1 - \Gamma_2/\Gamma_i) \quad (6)$$

where π is the surface pressure in mN/m and Γ_2 is the surface excess at that concentration. In Figure 6, the surface coverage as

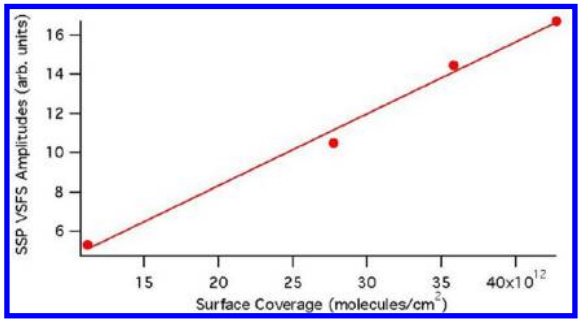

Figure 6. Plot of surface coverage versus fitted VSFS amplitude for SSP modes.

a function of bulk concentration of malonic acid is plotted as a function of the SSP VSFS fitted amplitudes. The linear dependence of the data and the unchanging frequency response in the C═O VSFS (SSP and SPS) data confirms that additional adsorption that occurs at the surface does not significantly change the orientation of the carboxylic C═O modes, but merely increases the total number of oscillators at the surface.

By combining the VSFS spectra and the surface tension data, a rudimentary picture of malonic acid adsorption at an aqueous interface can be drawn. According to the SSP data, there are carboxylic C═O oscillators oriented normal to the surface. According to the SPS data, there are also carboxylic C═O oscillators in the plane of the interface. This latter signal is less intense, potentially because of orientational averaging. These carboxylic C═O frequencies are indicative of very weak solvation. As the concentration of malonic acid is increased in the bulk, the surface concentration also increases, but in a fashion that does not alter the overall orientation of the C═O oscillators. This conclusion is supported by the surface tension data and the lack of changes in both the frequency and Gaussian width of the malonic acid C═O spectra as a function of concentration. The H_2O/CH region provides further evidence of adsorption that does not fully disrupt the topmost surface layer and that more strongly affects the hydrogen-bonding coordination. The lack of CH_2 signal is most likely due to an orientational averaging effect. These results therefore indicate isolated malonic acid molecules adsorbed to the very top of the air/water interface.

3.3. Effect of pH on Malonic Acid Adsorption.

3.3.1. Spectroscopic Results. The previous section investigated the adsorption characteristics of malonic acid as a function of concentration. Because malonic acid is a diprotic acid, the protonation state of the adsorbed species is necessary to fully describe the adsorption characteristics. As the pH is adjusted, the protonated carboxylic acid will turn into a resonance-stabilized carboxylate ion that completely removes the carboxylic C═O spectral response in this region. Because there are two carboxylic moieties, there are correspondingly two pK_a values. Based on IR bulk studies,[45] the frequency of the singly protonated carbonyl should be red-shifted as compared to that of the fully protonated species. Therefore, as the bulk pH is adjusted, malonic acid adsorbed at the interface can be examined for spectral changes indicating deprotonation. This will, in turn, provide more insight into the bonding environment at the interface.

The pK_a values for malonic acid are 2.85 and 5.70.[67] The percentages of protonated species for the bulk are plotted in Figure 7. At a pH of 3, the bulk percentage of fully protonated malonic acid should approach 40%, with the singly protonated form near 60%. At a pH of 4, the fully protonated form should be about 7%, with the singly protonated form at 91%, and the completely dissociated form near 2%. At a pH of 6, the fully protonated form should not exist, with a third of the acid

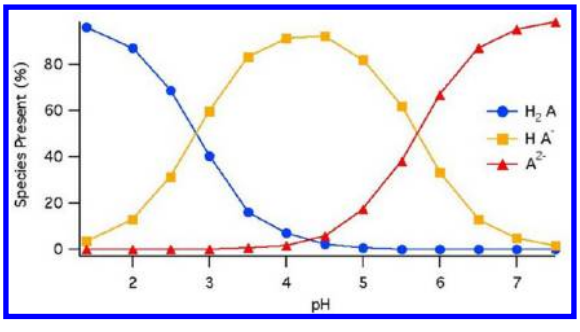

Figure 7. Plot of bulk percentages of fully protonated, singly protonated, and fully deprotonated malonic acid species.

dx.doi.org/10.1021/jp310851j | J. Phys. Chem. A 2013, 117, 2529−2542

molecules being singly protonated and the remaining two-thirds completely dissociated.

At a constant concentration of acid (1 M), the bulk pH was adjusted, and fitted spectra of the C═O region were recorded in both SSP and SPS schemes. Figure 8 shows the spectral response of malonic acid in the C═O region as a function of bulk adjusted pH, along with spectral fits. The SSP-active C═O mode is located at 1741 ± 2 cm^{-1} with a Gaussian width of 28 ± 1 cm^{-1}, whereas the SPS-active C═O mode is located at 1731 ± 2 cm^{-1} with a Gaussian width of 35 ± 1 cm^{-1}. The VSFS signal of the C═O mode decreased as the bulk adjusted pH was increased but did not track the bulk pK_a values closely. At a bulk pH value of 3, the SSP scheme (Figure 8a) gave signal with fitted amplitude that, although decreased compared to that of the non-pH-adjusted solutions, was still clearly present. In the SPS scheme (Figure 8b), the signal at pH 3 was very low and difficult to obtain. The SSP VSFS amplitudes continued to decrease, and by a pH of 6, the signal was nearly undetectable.

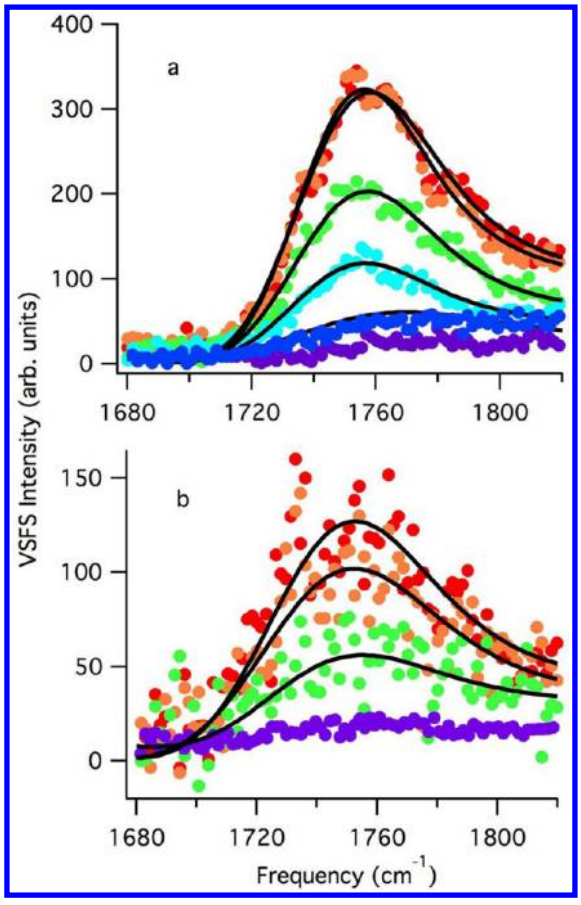

Figure 8. VSFS spectra of the carboxylic C═O mode of aqueous malonic acid (a) for SSP at 1 M with bulk adjusted pH values from native (top) to 6 (bottom) and (b) for SPS at 1 M with bulk adjusted pH values from native (top) to 6 (bottom).

Attempts were made to probe the COO^- region of malonic acid (~1400 cm^{-1}), but no signal could be found for native pH, pH 4, or pH 7 solutions. Detection of signal for a native pH solution would be unlikely because such a solution is dominated by the fully protonated species and, thus, very little carboxylate exist. Likewise, signal for pH 7 is unlikely because, although the solution is dominated by doubly deprotonated species, the surface tension indicates no adsorption to the interface. According to surface tension measurements addressed in the next section and C═O SSP VSFS measurements, malonic acid is still present at the interface at pH 4. At this pH, over 90% of the molecules (in the bulk) should be in the singly protonated state, and therefore, signal at pH 4 should be present if there are molecules at the interface. A lack of signal leads to two possibilities: (1) there is no orientational order for a singly or doubly deprotonated species at the interface or (2) desorption occurs when malonic acid loses a proton. Although it is difficult to distinguish between these two options, the invariant frequency in the C═O region as a function of pH would suggest that there is no change to the adsorbed species and, therefore, that the lack of signal is due to the inability of the mono- or dianion to remain at the interface. This would then indicate that malonic acid actually has a single pK_a value when it is at the surface and that the surface-active species is fully protonated malonic acid.

3.3.2. Surface Tension of Bulk pH-Adjusted Malonic Acid. To the best of our knowledge, this section constitutes the first published study of the surface tension of bulk pH-adjusted malonic acid solutions. Surface pressure (left axis) values and the square root of VSFS fitted amplitudes (right axis) are plotted as functions of bulk pH in Figure 9. It is known that NaOH can increase the surface pressure at the air/water interface,[68] so the surface pressure values plotted are corrected not by pure H_2O, but by H_2O with the equivalent NaOH added for each corresponding pH value. As the bulk pH was increased, the corrected surface pressure decreased. The surface pressure values were found to follow the square root of the VSFS fitted amplitudes, indicating that, as the bulk pH was adjusted to higher values, malonic acid was desorbing from the surface. If one recalls the bulk pK_a values and the corresponding percentages of species (Figure 7), it is clear that both the VSFS and surface pressure values closely followed the percentage of the fully protonated species. When combined with unchanging frequencies of the SSP- and SPS-active modes and the lack of a detectable COO^- signal, these results demonstrate that the surface-active species of malonic acid is the fully protonated form.

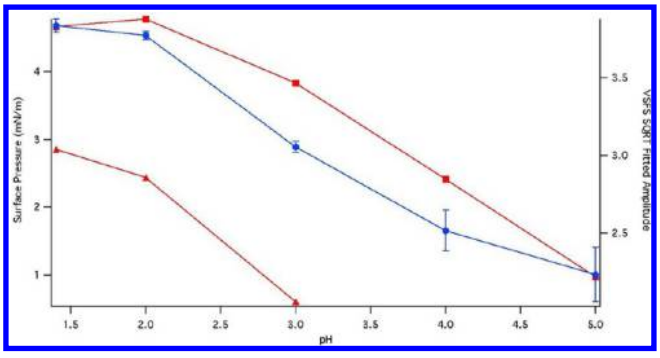

Figure 9. Plot of surface pressure (left axis) and square root of fitted VSFS amplitude for SSP and SPS C═O modes (right axis) versus pH for bulk pH-adjusted 1 M malonic acid.

The results of the concentration- and pH-dependent spectroscopic and surface tension studies provide an almost complete picture of the adsorption of malonic acid at the air/water interface. As the bulk concentration is increased, malonic acid does not change its orientation because of increased adsorption at the interface. There are two carboxylic acid moieties present at the interface, with the higher-energy moiety

dx.doi.org/10.1021/jp310851j | J. Phys. Chem. A 2013, 117, 2529−2542

having its dipole pointing perpendicular to the interface and the lower-energy moiety oriented in the plane of the bulk. It has been shown that probing these two distinct moieties by adjusting the bulk pH of the solutions results in no observed red shift of the C═O mode for either polarization scheme. In addition, the fully protonated species has been shown to be the surface-active species, indicating that the surface has only one pK_a value. VSFS does provide orientation information; however, because the VSFS studies here were not phase-sensitive, it was not possible to determine whether the dipole oscillators probed by the SSP polarization scheme were pointing into the vapor phase or into the aqueous phase. Phase-sensitive sum frequency generation[69] has been demonstrated to be capable of determining both the real and imaginary components of $\chi^{(2)}$ and, therefore, the unique phase associated with a resonance. By knowing the phase, the absolute orientation of a particular mode can be determined experimentally. However, the material of choice to create the local oscillator necessary for these experiments has traditionally been quartz. The use of this material is excluded in the carbonyl wavelength regions (~6 um) because of the lack of transmission of z-cut quartz. Although these experimental challenges might be remedied soon, the use of phase-sensitive sum frequency measurements is not possible for these experiments at this time. By probing the behavior of these molecules using computational methods, further information about the most likely geometries of malonic acid adsorption can be obtained and compared with the VSFS data, and a more complete picture of the bonding environment at the surface can be obtained without requiring phase-sensitive measurements.

4. COMPUTATIONAL MODELING OF MALONIC ACID ORIENTATION

4.1. Angle Descriptions of Chemical Moieties. A discussion of the molecular orientation of malonic acid begins with a description of the angles used in the following analyses. Because the carbon atoms form the backbone of the malonic acid molecular structure, determining the orientation of the three atoms is the first step in understanding the overall orientation of the molecule in space with respect to a water surface. The orientation of the carbon chain backbone is described using two angles, and the molecule is oriented internally using two dihedral angles. All of the angle definitions described in this section are depicted in Figure 10.

The group of three carbon atoms forms a moiety with C_{2v} symmetry. The two C—C bond vectors have a bisector between them. In this work, the bisector is always referred to as a vector pointing from the central carbon in the direction of the other two carbon atoms. The first angle defined, θ, describes the "tilt" of the triatomic carbon chain that forms the acid's backbone. The angle θ is calculated as the angle formed between the carbon group bisector vector and a reference axis oriented perpendicularly to the water surface, pointing from the water bulk toward the gas-phase side of the water interface. When $\theta = 0°$, the bisector vector aligns with the reference axis. A value of $\theta = 90°$ places the bisector vector in the plane of the water surface, perpendicular to the reference axis. Rotating the bisector to $\theta = 180°$ makes the bisector antialigned with the reference axis, pointing in toward the water side of the interface.

The second angle used to orient the malonic acid carbon backbone, φ, describes a molecular "twist" of the malonic acid. This twist angle is defined as a rotation of the plane formed by the three carbon atoms around the bisector axis. For different orientations of the angle φ, the distribution of φ will necessarily become isotropic because of the symmetries of the plane of the aqueous slab surface. However, the value of φ is necessary to describe the overall molecular orientation for θ values near 90°. When $\theta = 90°$, the bisector of the carbon atom group lies parallel to the water surface. In such a configuration, $\varphi = 0°$ means the plane of the carbon atoms orient perpendicularly to the plane of the water surface. Likewise, $\varphi = 90°$ lays the plane of the carbon atom group at on the surface, parallel to the plane of the water interface.

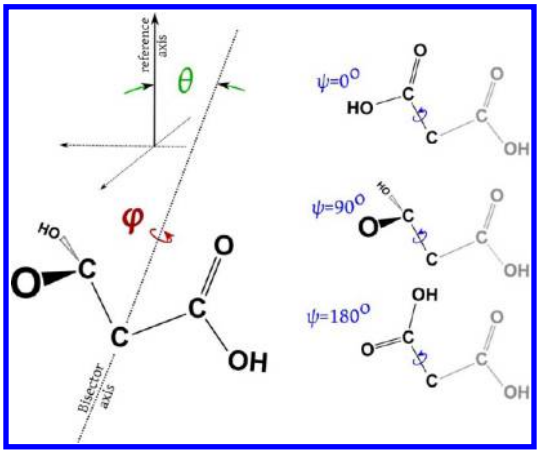

Figure 10. Description of angles that are used to orient a malonic acid molecule both in the space-fixed frame and internally in the molecular frame. θ (green) is the tilt, φ (red) is the twist, and ψ (blue) represents two dihedral angles. Three values of ψ are depicted at the right.

The planes formed by the atoms of the carboxylic acid groups are oriented by rotation of two dihedral angles, collectively referred to as ψ because they are not uniquely identified, referenced to the plane of the three backbone carbon atoms. The dihedral angle is the angle of rotation of the C—C bond between the central methylene carbon and a carbonyl carbon of a carboxylic acid moiety. The reference orientation that sets $\psi = 0°$ is defined by two conditions: (1) the plane of the atoms of the carboxylic acid is oriented parallel to the plane of the three carbon atoms, and (2) the carbonyl C═O bond vector (pointing from the C to the O) points to the same side as the C—C—C bisector vector (i.e., the inner product of the bisector vector and the carbonyl bond vector has a positive value: C═O·bisector > 0). A dihedral angle of $\psi = 90°$ rotates the O═C—O plane perpendicular to the C—C—C plane. Lastly, $\psi = 180°$ rotates the carboxylic acid such that the carbonyl is antialigned with the C—C—C bisector. The various orientations of the dihedral angles are depicted in Figure 10 and characterize the internal orientation of malonic acid. By combining all three of the described angles with information about the acid position within the simulation box, one can develop a complete picture of the orientational behavior of malonic acid relative to a nearby water surface.

4.1. Carbon Backbone Orientation. Bivariate angle distributions of θ and φ were calculated for the three carbon backbone atoms and are shown in Figure 11. The set of plots represents slices through the interface parallel to the water surface. Each slice is located at the distance labeled in the top right of the respective plot. Positive positions are farther into the vacuum phase, and negative positions are farther into the aqueous phase of the interface. A distance of 0 Å is located at the water surface location. The location of the surface and all

dx.doi.org/10.1021/jp310851j | J. Phys. Chem. A 2013, 117, 2529−2542

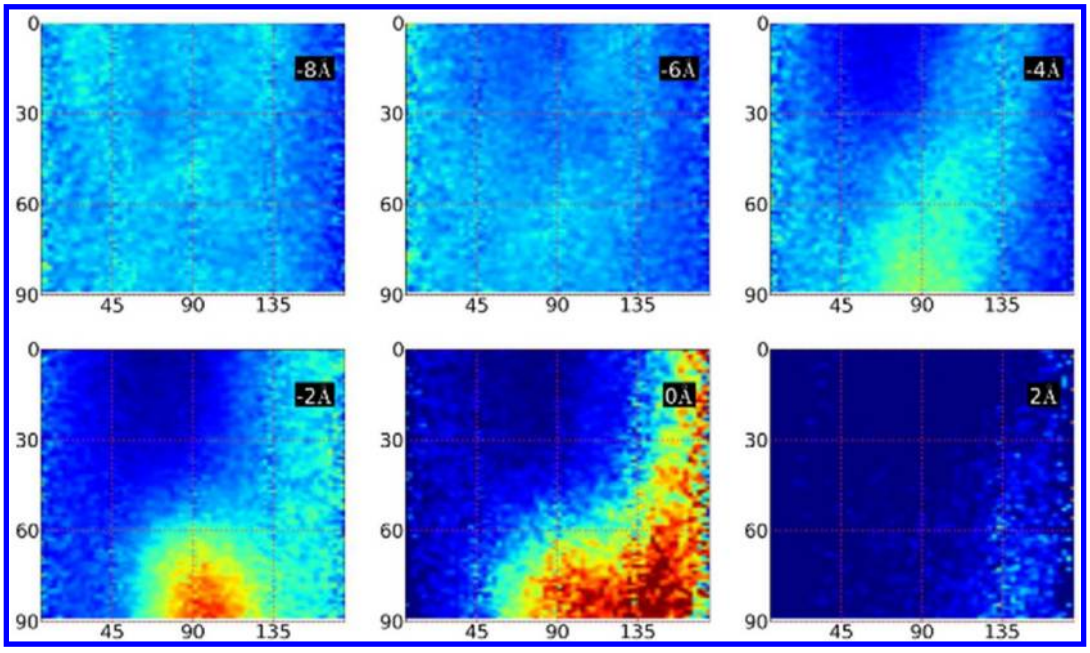

Figure 11. Bivariate distribution plot of the tilt (θ) and twist (φ) of the malonic acid carbon chain, with each plot representing a 2-Å slice of the simulated aqueous slab at the indicated depth.

calculations performed to relate interfacial position were accomplished using a method of averaging topmost water molecule positions, fully described in a previous publication.[44] The molecular center of mass determined the position of each malonic acid molecule.

In each set of axes in Figure 11, the values of θ and φ are plotted along the horizontal and vertical directions, respectively. The plots are two-dimensional histograms colored by the intensity (i.e., population) of the location in the angle space. Higher intensity is colored dark red, and lower intensity is dark blue. Areas in the plots characterized by uniform coloration indicate an isotropic distribution of angles. A concentrated region of uniform coloration indicates an orientational preference in one or both of the angular degrees of freedom.

The plots for interface positions of 2 Å in Figure 11 show the orientation of the acid carbon backbones just above the water surface. The plot intensities at these positions of the interface indicate the presence of malonic acid and correspond to the surface adsorption behavior found in the VSFS experiments. These acid molecules are most likely less solvated than those farther into the water bulk. The most distinguishing feature is the vertically running band of intensity to the right of the plot centered between 135° and 180°. This results from a population of acid molecules with their three carbon atoms oriented with the carbon-group bisector vector pointed more than 45° into the water bulk. φ is spread nearly isotropically in this distribution. However, because of the symmetry of the θ angle as a spherical coordinate (i.e., a single θ value describes a cone in space), φ will necessarily become more isotropic relative to the interface, or spread out across the two-dimensional plots, as θ takes values near its extrema. Values of θ closer to 90° require φ to fully describe the orientation.

At 0 Å and below, the acid carbon backbone orientations are more complex. A second population of orientations forms at 0 Å, manifested in the plots as a region of intensity centered at θ = 90°, with φ also concentrated toward 90°. This indicates a carbon atom group lying flat in the plane of the water surface. Additionally, as the depth of the molecules increases from 0 to −4 Å, the population above θ = 135° decreases, shifting intensity to the peak at θ = 90°. The distribution spreads out in both θ and φ. For acid molecules deeper into the water bulk, likely more solvated by water molecules, the orientational freedom expands in θ and φ until, at −6 Å, there is a loss of orientational preference, resulting in a flat (evenly colored) distribution and isotropy of the orientation of the carbon backbone group.

At −4 Å, the distribution expands below θ = 45°. This is due to a population of submerged malonic acid molecules with their bisectors aimed slightly up toward the water surface. Thus, it is established that the influence of the interface on molecular orientation extends both above and below the water surface and extends to a depth of at least 4 Å into the bulk water.

4.2. CH_2 Orientation. For each acid molecule, the orientation θ of the carbon backbone affects the position and orientation of the molecule's methylene hydrogens. For an orientation of θ = 90°, and for all φ values, there are two hydrogens (one from each methylene) in a rather symmetrical configuration with one above and one below the backbone's plane, which is itself parallel to the plane of the water interface. With θ = 90°, variation in φ results in the plane formed by each H—C—H moiety rotating from perpendicular (φ = 0°) to parallel (θ = 90°) to that of the water surface. Consider acid orientations near θ = 90° and further consider the vector defined by each methylene's C—H bond. The geometry of the acid is such that each of these C—H bond vectors has a component perpendicular to the plane of the interface and the magnitude of each vector's perpendicular component is identical. Effectively, these "perpendicular-to-the-water-interface" components are mirrors of each other.

Furthermore, if the θ distribution is symmetric around θ = 90° (as in the −2 Å plot of Figure 11), then the perpendicular components of the two methylene C—H bonds negate each other. The carbon group θ–φ distributions at or below the water surface (≤0 Å) exhibit this quality. The VSFS experiments failed to produce any spectral features related to the methylene CH_2 modes of malonic acid. Thus, it is proposed

dx.doi.org/10.1021/jp310851j | J. Phys. Chem. A 2013, 117, 2529−2542

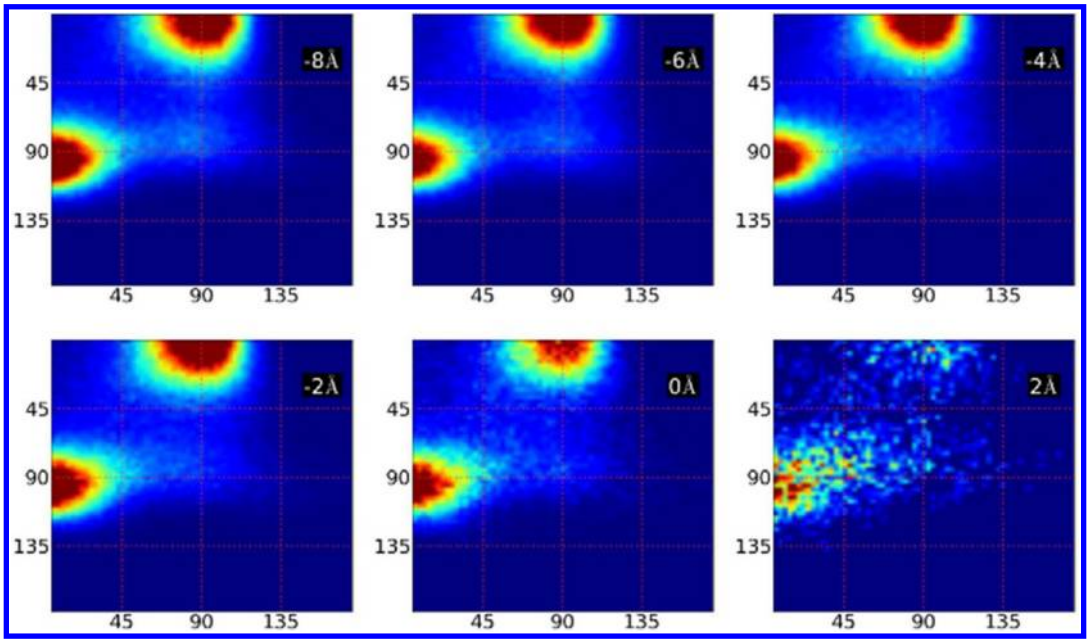

Figure 12. Internal orientation of malonic acid as a function of dihedral angles, ψ, describing the angle formed between the plane of the O═C—O atoms of the carboxylic acid group and the plane of the three carbon atoms. Each plot represents a 2-Å slice of the simulated aqueous slab at the indicated depth.

that the aforementioned orientational symmetry of the methylene C—H bonds about the water surface and the low population of malonic acid molecules above the surface location manifest spectrally in the polarized VSFS experiments as a lack of intensity where the C—H bond features are expected.

4.3. Carbon Backbone Dihedral Angles. Having established the orientation of the carbon backbone atom group from the distributions in Figure 11, the analysis of the internal geometry of carboxylic acid moieties near the water surface was explored. The two carboxylic acid groups rotate around the two C—C bonds, quantified by their dihedral angles. The magnitudes of the dihedral angles fall in the range $0° \leq \psi \leq 180°$. The O═C—O atomic plane is parallel to the C—C—C plane at $\psi = 0°$ and $\psi = 180°$, and the two planes are perpendicular at $\psi = 90°$, as discussed above and depicted in Figure 10. The two dihedral angles are plotted in a set of bivariate distributions in Figure 12. The arrangement of the axes in this figure is identical to that in Figure 11, but with each axis representing one of the two ψ angles.

Figure 12 shows that the dihedral orientations are strongly related with a preferred rotation of 90° apart from each other. The two very concentrated peaks in the plots are located at $\psi = 0°$ and $\psi = 90°$. This results from the carboxylic O═C—O atomic planes of the two carboxylic acid molecules aligning perpendicularly to each other. The topmost plot at 2 Å is not symmetric between the two dihedral angles, with only a single peak in the distribution (located at the left center of the axis). This is an artifact of how the carboxylic acid groups were enumerated computationally and indicates that the topmost malonic acid molecules above the water surface take on a fixed dihedral orientation, rarely switching values (i.e., rotating the molecule to flip the alignment of both carboxylic acid groups).

One of the carbonyl C═O bonds is preferentially aligned in the same direction as the carbon group bisector ($\psi = 0°$) and in the plane of the three carbons. The other carbonyl C═O bond points perpendicular to the plane of the carbon group atoms. The strong orientational preference was observed both in the bulk of the water and at the water surface location. This difference between the two carboxylic group orientations likely manifests spectrally as a shifting of the carbonyl peak frequencies. Each end of the molecule is configured differently and is likely located in different solvation environments. The spectral peak shifting of the two polarization schemes of the VSFS experiments results directly from the orientational preferences of the two carboxylic acid groups of the malonic acid molecule.

There remains one final set of orientational data necessary to fully characterize the interfacial malonic acid. The θ–φ distributions of the carbon atoms show that the acid carbon chain lies flat when at the water surface (0 Å) and tilts with the bisector pointing farther into the water bulk when the malonic acid is slightly above the water surface. The ψ–ψ dihedral distributions show one C═O carbonyl bond mostly aligned with the carbon group bisector and the other carbonyl aligned normal to the plane of the carbon atoms. The question remains as to the direction in which the latter carbonyl C═O bond vector points: Is it pointed into the water side of the interface, or does it point out toward the gas phase away from the water bulk?

The carbonyl orientation was determined by calculating the tilt angle of the C═O bond, $\theta_{C=O}$. Similarly to the carbon group bisector tilt angle, $\theta_{C=O}$ is referenced to the axis normal to the plane of the water surface, pointing out toward the gas-phase side of the interface. Figure 13 shows the angle distribution of $\theta_{C=O}$ plotted as a function of the malonic acid molecular center-of-mass position. Most of the distribution is isotropic in the tilt angle up to positions several angstroms beneath the water surface location.

Starting above the surface (positions > 0 Å), the distribution bifurcates into two distinct angle regions. There is a protrusion in the distribution (region A in Figure 13) beginning just below 0 Å and extending above the surface, centered at $\theta_{C=O} = 90°$. A second peak in the distribution (region B) is concentrated toward the bottom of the plot near $\theta_{C=O} = 180°$. At this

dx.doi.org/10.1021/jp310851j | J. Phys. Chem. A 2013, 117, 2529–2542

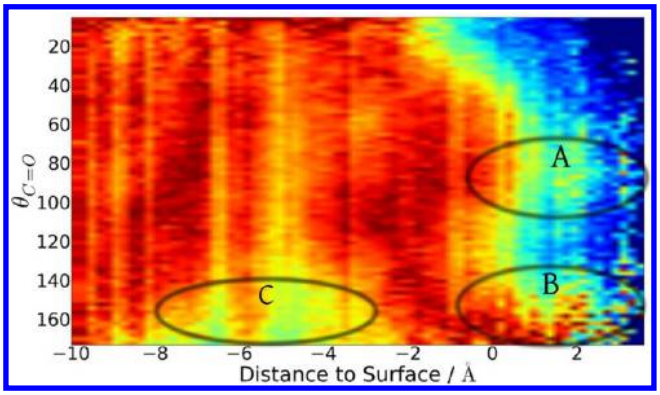

Figure 13. Two-dimensional histogram of the carbonyl bond tilt angle $\theta_{C=O}$ plotted against the molecular center-of-mass position.

position slightly above the water surface, it is more clear that one of the carbonyl C═O bonds points into the water (the bond oriented near $\theta_{C=O}$ = 180°) and the other points more outward into the plane of the surface and often slightly angled outward from the water phase. When an acid molecule located at, or just above, the water interface exhibits this internal orientation, it means that one carbonyl bond is oriented pointing more toward bulk water while the other is oriented pointing toward the gas phase.

The MD data provide a direct determination of the microscopic geometries of the interfacial molecules. Extrapolating the same orientational information from VSFS makes use of phase parameters extracted from the spectral fitting. The VSFS experiments were not performed using phase-sensitive techniques; thus, conclusions regarding the orientation of complex molecular modes do not account for the signs of the elements of the molecular hyperpolarizabilities and require further calculations to draw conclusions about absolute orientation.[70] Short of performing the calculation of each hyperpolarizability tensor element of the carboyxlic acid groups, the use of MD is necessary to draw any conclusions about the absolute orientations of the various modes of malonic acid. The results of these calculations are consistent with the spectroscopic assignments from the experiments.

Farther down into the water surface, the angle distribution spreads over a much larger range until becoming isotropic near −2 Å. However, a feature appears at −3 Å and extends down slightly past −8 Å into the water phase (region C in Figure 13). In this region, there is a decreased intensity in the histogram for $\theta_{C=O}$ > 120°. This shows a population of malonic acid carbonyl C═O bonds pointing less into the bulk water. At this depth, the carbon backbone orientation distribution becomes relatively more isotropic, but there remains a population of acid molecules with θ_{CCC} < 90° (i.e., the carbon group bisector aims further toward the water surface), in agreement with the carbonyl bond behavior and the carboxylic dihedral orientations.

These orientational distributions paint the following picture of malonic acid orientation broken into interfacial depth regions: (1) Above the water surface, the carbon group bisector tilts down toward the water, and the carbonyl bonds orient with one bond pointing toward the water phase and the other pointing out of the water either parallel to the plane of the surface or slightly out toward the gas phase. (2) At the water surface location (0 Å), the carbon group lies mostly flat in the plane of the surface. The methylene C—H bonds align symmetrically above and below the surface. Also, the carbonyl C═O bonds have an orientation similar to those farther out of the water, but the carbonyl bond tilt distribution quickly becomes isotropic just a few angstroms under the surface location. (3) At −4 Å and to approximately −6 Å, the carbon group θ–φ distributions broaden and quickly become isotropic. The distribution of the carbonyl bond tilt, $\theta_{C=O}$, shifts intensity at this lower depth, leaving a low-intensity region at approximately 120° ≤ $\theta_{C=O}$. Both carbonyl groups orient to point more toward the water surface at this depth than slightly above or below. (4) Farther down in the water bulk, below −8 Å, the distributions become isotropic, and malonic acid assumes bulk-like behavior. The outstanding correlation between the MD results and the experimental results provides confidence in the spectral assignments. The combined use of MD and experiments therefore builds a complete picture of the adsorption of malonic acid to the air/water interface.

The results from this study point to a unique geometry at the air/water interface for malonic acid: an intramolecularly bonded ring structure. In this ring structure, which has been seen before in computational studies of gas-phase malonic acid,[71,72] the OH mode associated with SSP-active C═O is hydrogen-bonded to the SPS-active C═O to form a stable six-membered ring. This structure provides an explanation for the frequency differences in the SSP and SPS VSFS spectra of C═O, the strong OH bonding seen in the SSP VSFS spectra of the OH/CH region, the weak solvation at the interface, and the pH dependence. Preliminary MD evidence has shown this structure to be stable at the air/water interface, and calculations are currently being performed to confirm this structure.

5. CONCLUSIONS

By using vibrational sum frequency spectroscopy, surface tension measurements, and MD calculations, the adsorption and orientation of malonic acid to the air/water interface has been fully described. VSFS results in the C═O region demonstrate that carboxylic C═O oscillators have frequencies representative of weak solvation at the air/water interface, whereas VSFS results in the OH region confirm results from surface pressure experiments that malonic acid does not fully saturate the surface. The VSFS and surface tension studies also clearly show that the orientation of the adsorbed malonic acid molecules does not change as a function of concentration. pH studies of malonic acid adsorption demonstrate that the surface-active species of malonic acid is the fully protonated species. Computational results confirm and enhance the conclusions from the VSFS results and provide quantifiable distributions of malonic acid orientation as a function of depth into the water surface.

These results paint a picture of an isolated malonic acid molecule that lies mostly flat on the surface of an aqueous solution and displays no acid–acid interactions at the surface. There is a competition at the interface for the hydrophobic alkane spacer between the two carboxylic ends to remove itself from the water while still allowing the hydrophilic carboxylic ends to be solvated by aqueous-phase water molecules. As a result, surface malonic acid is not well solvated, and the surface-active species are located in the first layer of water molecules. Malonic acid molecules just a few angstroms deeper into the aqueous phase assume bulk-like behavior. The weak solvation is also apparent due to the fact that the aqueous surface cannot accommodate malonic acid molecules that are partially or completely deprotonated.

dx.doi.org/10.1021/jp310851j | J. Phys. Chem. A 2013, 117, 2529–2542

Organic compounds found in atmospheric aerosols frequently include significant amounts of dicarboxylic acids, and these polar compounds are predominantly in condensed phases because of their low vapor pressures. In addition, dicarboxylic acids have been shown to be viable cloud condensation nuclei (CCN). As the surface-to-volume ratio of these aerosol systems can be very large, it is exceedingly necessary to understand the properties of these molecules at an air/water interface. This study provides a complete picture of the adsorption, speciation, and orientation of malonic acid. These results also demonstrate that the pH of an aerosol can have an effect on the surface speciation of malonic acid and, correspondingly, the total number of acidic protons available at an aerosol surface, with obvious implications for heterogeneous reactions that can occur at the surface of an aerosol.

AUTHOR INFORMATION

Corresponding Author

*Tel.: 541-346-4635. Fax: 541-346-5859. E-mail: richmond@uoregon.edu.

Notes

The authors declare no competing financial interest.

ACKNOWLEDGMENTS

The authors thank the National Science Foundation (Grant CHE-1051215) for support of this research.

REFERENCES

(1) Seinfeld, J. H.; Pandis, S. N. *Atmospheric Chemistry and Physics*; Wiley-Interscience: New York, 1998.
(2) Finlayson-Pitts, B. J.; Pitts, J. N. *Chemistry of the Lower and Upper Atmosphere*; Academic Press: San Diego, CA, 2000.
(3) Chebbi, A.; Carlier, P. Carboxylic Acids in the Troposphere, Occurrence, Sources, and Sinks: A Review. *Atmos. Environ.* **1996**, *30*, 4233−4249.
(4) Kawamura, K.; Usukura, K. Distributions of Low Molecular Weight Dicarboxylic Acids in the North Pacific Aerosol Samples. *J. Oceanogr.* **1993**, *49*, 271−283.
(5) Kawamura, K.; Kasukabe, H.; Barrie, L. A. Source and Reaction Pathways of Dicarboxylic Acids, Ketoacids and Dicarbonyls in Arctic Aerosols: One Year of Observations. *Atmos. Environ.* **1996**, *30*, 1709−1722.
(6) Kawamura, K.; Sakaguchi, F. Molecular Distributions of Water Soluble Dicarboxylic Acids in Marine Aerosols over the Pacific Ocean Including Tropics. *J. Geophys. Res.* **1999**, *104*, 3501−3509.
(7) Sempéré, R.; Kawamura, K. Comparative Distributions of Dicarboxylic Acids and Related Polar Compounds in Snow, Rain, and Aerosols from Urban Atmosphere. *Atmos. Environ.* **1994**, *28*, 449−459.
(8) Sempéré, R.; Kawamura, K. Low molecular weight dicarboxylic acids and related polar compounds in the remote marine rain samples collected from western Pacific. *Atmos. Environ.* **1996**, *30*, 1609−1619.
(9) Aggarwal, S. G.; Kawamura, K. Molecular Distributions and Stable Carbon Isotopic Compositions of Dicarboxylic Acids and Related Compounds in Aerosols from Sapporo, Japan: Implications for Photochemical Aging during Long-Range Atmospheric Transport. *J. Geophys. Res.* **2008**, *113*, 13.
(10) Hsieh, L.-Y.; Kuo, S.-C.; Chen, C.-L.; Tsai, Y. I. Origin of Low-Molecular-Weight Dicarboxylic Acids and Their Concentration and Size Distribution Variation in Suburban Aerosol. *Atmos. Environ.* **2007**, *41*, 6648−6661.
(11) Hsieh, L.-Y.; Kuo, S.-C.; Chen, C.-L.; Tsai, Y. I. Size Distributions of Nano/micron Dicarboxylic Acids and Inorganics Ions in Suburban PM Episode and Non-Episodic Aerosol. *Atmos. Environ.* **2009**, *43*, 4396−4406.
(12) Pavuluri, C. M.; Kawamura, K.; Swaminathan, T. Water-Soluble Organic Carbon, Dicarboxylic Acids, Ketoacids, and α-Dicarbonyls in the Tropical Indian Aerosols. *J. Geophys. Res.* **2010**, *115*, 15.
(13) Parsons, M. T.; Mak, J.; Lipetz, S. R.; Bertram, A. K. Deliquescence of Malonic, Succinic, Glutaric, and Adipic Acid Particles. *J. Geophys. Res.* **2004**, *109*, 8.
(14) Braban, C. F.; Carroll, M. F.; Styler, S. A.; Abbatt, J. P. D. Phase Transitions of Malonic and Oxalic Acid Aerosols. *J. Phys. Chem. A* **2003**, *107*, 6594−6602.
(15) Hansen, A. R.; Beyer, K. D. Experimentally Determined Thermochemical Properties of the Malonic Acid/Water System: Implications for Atmospheric Aerosols. *J. Phys. Chem. A* **2004**, *108*, 3457−3466.
(16) Hyvärinen, A.-P.; Lihavainen, H.; Gaman, A.; Vairila, L.; Ojala, H.; Kulmala, M.; Viiasnen, Y. Surface Tensions and Densities of Oxalic, Malonic, Succinic, Maleic, Malic, and *cis*-Pinonic Acids. *J. Chem. Eng. Data* **2006**, *51*, 255−260.
(17) Booth, A. M.; Topping, D. O.; McFiggans, G.; Percival, C. J. Surface Tension of Mixed Inorganic and Dicarboxylic Acid Aqueous Solutions at 298.15 K and Their Importance for Cloud Activation Predictions. *Phys. Chem. Chem. Phys.* **2009**, *11*, 8021−8028.
(18) Riipinen, I.; Koponen, I. K.; Frank, G. P.; Hyärinen, A.-P.; Vanhanen, J.; Lihavainen, H.; Lehtinen, K. E. J.; Bilde, M.; Markku, K. Adipic and Malonic Acid Aqueous Solutions: Surface Tensions and Saturation Vapor Pressures. *J. Phys. Chem. A* **2007**, *111*, 12995−13002.
(19) Varga, Z.; Kiss, G.; Hansson, H.-C. Modelling the Cloud Condensation Nucleus Activity of Organic Acids on the Basis of Surface Tension and Osmolality Measurements. *Atmos. Chem. Phys.* **2007**, *7*, 4601−4611.
(20) Giebl, H.; Berner, A.; Reischl, G.; Puxbaum, H.; Kasper-Giebl, A.; Hitzenberger, R. CCN Activation of Oxalic and Malonic Acid Test Aerosols with the University of Vienna Cloud Condensation Nuclei Counter. *J. Aerosol Sci.* **2002**, *33*, 1623−1634.
(21) Finlayson-Pitts, B. J. Reactions at Surfaces in the Atmosphere: Integration of Experiments and Theory as Necessary (But Not Necessarily Sufficient) for Predicting the Physical Chemistry of Aerosols. *Phys. Chem. Chem. Phys.* **2009**, *11*, 7760−7779.
(22) Hayase, S.; Yabushita, A.; Kawasaki, M.; Enami, S.; Hoffman, M. R.; Colussi, A. J. Weak Acids Enhance Halogen Activation on Atmospheric Water's Surfaces. *J. Phys. Chem. A* **2011**, *115*, 4935−4940.
(23) Gao, S. S.; Abbatt, J. P. D. Kinetics and Mechanism of OH Oxidation of Small Organic Dicarboxylic Acids in Ice: Comparison to Behavior in Aqueous Solution. *J. Phys. Chem. A* **2011**, *115*, 9977−9986.
(24) Tedetti, M.; Kawamura, K.; Charriére, B.; Chevalier, N.; Sempére, R. Determination of Low Molecular Weight Dicarboxylic and Ketocarboxylic Acids in Seawater Samples. *Anal. Chem.* **2006**, *78*, 6012−6018.
(25) Bertilsson, S.; Travnik, L. J. Photochemical Transformation of Dissolved Organic Matter in Lakes. *Limnol. Oceanogr.* **2000**, *45*, 753−762.
(26) Narukawa, M.; Kawamura, K.; Li, S.-M.; Bottenheim, J. W. Dicarboxylic Acids in the Arctic Aerosols and Snowpacks Collected during ALERT 2000. *Atmos. Environ.* **2002**, *36*, 2491−2499.
(27) Shen, Y. R. Exploring New Opportunities with Sum-Frequency Nonlinear Optical Spectroscopy. *Pure Appl. Chem.* **2001**, *73*, 1589−1598.
(28) Richmond, G. L. Molecular Bonding and Interactions at Aqueous Surfaces as Probed by Vibrational Sum Frequency Spectroscopy. *Chem. Rev* **2002**, *102*, 2693−2724.
(29) Jubb, A. M.; Hua, W.; Allen, H. C. Environmental Chemistry at Vapor/Water Interfaces: Insights from Vibrational Sum Frequency Generation Spectroscopy. *Annu. Rev. Phys. Chem.* **2012**, *63*, 107−130.
(30) Bain, C. D.; Davies, P. B.; Ong, T. H.; Ward, R. N. Quantitative Analysis of Monolayer Composition by Sum-Frequency Vibrational Spectroscopy. *Langmuir* **1991**, *7*, 1563−1566.
(31) Soule, M. C. K.; Blower, P. G.; Richmond, G. L. Effects of Atmospherically Important Solvated ions on Organic Acid Adsorption

at the Surface of Aqueous Solutions. *J. Phys. Chem. B* **2007**, *111*, 13703−13713.
(32) Soule, M. C. K.; Blower, P. G.; Richmond, G. L. Nonlinear Vibrational Spectroscopic Studies of the Adsorption and Speciation of Nitric Acid at the Vapor/Acid Solution Interface. *J. Phys. Chem. A* **2007**, *111*, 3349−3357.
(33) Ota, S. T.; Richmond, G. L. Chilling Out: A Cool Aqueous Environment Promotes the Formation of Gas−Surface Complexes. *J. Am. Chem. Soc.* **2011**, *133*, 7497−7508.
(34) Gragson, D. E.; Alavi, D. S.; Richmond, G. L. Tunable Picosecond Infrared Laser System Based on Parametric Amplification in KTP with a Ti:Sapphire Oscillator. *Opt. Lett.* **1995**, *20*, 1991−1993.
(35) Gragson, D. E.; McCarty, B. M.; Richmond, G. L.; Alavi, D. S. High-Power Broadly Tunable Picosecond IR Laser System for Use in Nonlinear Spectroscopic Investigations. *J. Opt. Soc. Am. B.* **1996**, *13*, 2075−2083.
(36) Allen, H. C.; Raymond, E. A.; Richmond, G. L. Surface Structural Studies of Methanesulfonic Acid at Air/Aqueous Solution Interfaces Using Vibrational Sum Frequency Spectroscopy. *J. Phys. Chem. A* **2001**, *105*, 1649−1655.
(37) Davies, J. T.; Rideal, E. K. *Interfacial Phenomena*, 2nd ed.; Academic Press: New York, 1963.
(38) Borkowski, M. *Base Acid Titration and Equilibria (BATE) pH calculator 1.0.3.15*; 2008.
(39) Case, D. A.; Darden, T. A.; Cheatham, T. E., III; Simmerling, C. L.; Wang, J.; Duke, R. E.; Luo, R.; Walker, R. C.; Zhang, W.; Merz, K. M.; Roberts, B.; Wang, B.; Hayik, S.; Roitberg, A.; Seabra, G.; Kolossváry, I.; Wong, K. F.; Paesani, F.; Vanicek, J.; Liu, J.; Wu, X.; Brozell, S. R.; Steinbrecher, T.; Gohlke, H.; Cai, Q.; Ye, X.; Wang, J.; Hsieh, M.-J.; Cui, G.; Roe, D. R.; Mathews, D. H.; Seetin, M. G.; Sagui, C.; Babin, V.; Luchko, T.; Gusarov, S.; Kovalenko, A.; Kollman, P. A. *AMBER 11*; University of California, San Francisco, CA, 2010.
(40) Pearlman, D. A.; Case, D. A.; Caldwell, J. W.; Ross, W. S.; Cheatham, T. E., III; Debolt, S.; Ferguson, D.; Seibel, G.; Kollman, P. AMBER, a package of computer programs for applying molecular mechanics, normal mode analysis, molecular dynamics and free energy calculations to simulate the structural and energetic properties of molecules. *Comput. Phys. Commun.* **1995**, *91*, 1−41.
(41) Martinez, L.; Andrade, R.; Birgin, E.; Martinez, J. PACKMOL: A Package for Building Initial Configurations for Molecular Dynamics Simulations. *J. Comput. Chem.* **2009**, *30*, 2157−2164.
(42) Caldwell, J. W.; Kollman, P. A. Structure and Properties of Neat Liquids Using Nonadditive Molecular Dynamics: Water, Methanol, and *N*-Methylacetamide. *J. Phys. Chem.* **1995**, *99*, 6208−6219.
(43) Case, D. A.; Cheatham, T. E., III; Darden, T.; Gohlke, H.; Luo, R.; Merz, K. M.; Onufriev, A.; Simmerling, C.; Wang, B.; Woods, R. J. The Amber Biomolecular Simulation Programs. *J. Comput. Chem.* **2005**, *26*, 1668−1688.
(44) Shamay, E. S.; Johnson, K.; Richmond, G. L. Dancing on Water: The Choreography of Sulfur Dioxide Adsorption to Aqueous Surfaces. *J. Phys. Chem. C* **2011**, *115*, 25304−25314.
(45) Cabaniss, S. E.; Leenheer, J. A.; McVey, I. F. Aqueous Infrared Carboxylate Absorbances: Aliphatic Di-acids. *Spectrochim. Acta A* **1998**, *54*, 449−458.
(46) Socrates, G. *Infrared Characteristic Group Frequencies*, 2nd ed.; Wiley Interscience: Chichester, U.K., 1994.
(47) Gericke, A.; Huhnerfuss, H. In Situ Investigations of Saturated Long-Chain Fatty Acids at the Air/Water Interface by External Infrared Reflection-Absorption Spectroscopy. *J. Phys. Chem.* **1993**, *97*, 12899−12908.
(48) Johann, R.; Vollhardt, D.; Mohwald, H. Study of the pH Dependence of Head Group Bonding in Arachidic Acid Monolayers by Polarization Modulation Infrared Reflection Absorption Spectroscopy. *Colloids Surf. A* **2001**, *182*, 311−320.
(49) Wolfs, I.; Dessyn, H. O. Characteristic Vibrational Pattern for the Cyclic Dimer Carboxylic Acid Function in the Solid State. *Appl. Spectrosc.* **1996**, *50*, 1000−1006.
(50) Ghorai, S.; Laskin, A.; Tivanski, A. V. Spectroscopic Evidence of Keto−Enol Tautomerism in Deliquesced Malonic Acid Particles. *J. Phys. Chem. A* **2011**, *115*, 4373−4380.
(51) Lambert, A. G.; Davies, P. B.; Neivandt, D. J. Implementing the Theory of Sum Frequency Generation Vibrational Spectroscopy: A Tutorial Review. *Appl. Spectrosc. Rev.* **2005**, *40*, 103−145.
(52) Johnson, C. M.; Tyrode, E.; Baldelli, S.; Rutland, M. W.; Leygraf, C. A Vibrational Sum Frequency Spectroscopy Study of the Liquid−Gas Interface of Acetic Acid−Water Mixtures: 1. Surface Speciation. *J. Phys. Chem. B* **2005**, *109*, 321−328.
(53) Sovago, M.; Campen, R. K.; Bakker, H. J. Hydrogen Bonding Strength of Interfacial Water Determined with Surface Sum-Frequency Generation. *Chem. Phys. Lett.* **2009**, *470*, 7−12.
(54) Raymond, E. A.; Tarbuck, T. L.; Brown, M. G.; Richmond, G. L. Hydrogen-Bonding Interactions at the Vapor/Water Interface Investigated by Vibrational Sum-Frequency Spectroscopy of HOD/H_2O/D_2O Mixtures and Molecular Dynamics Simulations. *J. Phys. Chem. B* **2003**, *107*, 546−556.
(55) Tian, C.-S.; Shen, Y. R. Isotopic Dilution Study of the Water/Vapor Interface by Phase-Sensitive Sum-Frequency Vibrational Spectroscopy. *J. Am. Chem. Soc.* **2009**, *131*, 2790−2791.
(56) Buch, V. Molecular Structure and OH-Stretch Spectra of Liquid Water Surface. *J. Phys. Chem. B* **2005**, *109*, 17771−17774.
(57) Morita, A.; Hynes, J. T. A Theoretical Analysis of the Sum Frequency Generation Spectrum of the Water Surface. II. Time-Dependent Approach. *J. Phys. Chem. B* **2002**, *106*, 673−685.
(58) Walker, D. S.; Hore, D. K.; Richmond, G. L. Understanding the Population, Coordination, and Orientation of Water Species Contributing to the Nonlinear Optical Spectroscopy of the Vapor−Water Interface through Molecular Dynamics Simulations. *J. Phys. Chem. B* **2006**, *110*, 20451−20459.
(59) Ota, S. T. Vibrational Sum Frequency Spectroscopic Investigations of Sulfur Dioxide Adsorption to Atmospherically Relevant Aqueous Surfaces. Ph.D. Dissertation, University of Oregon, Eugene, OR, 2011.
(60) Lin-Vien, D.; Colthup, N. B.; Fateley, W. G.; Grasselli, J. G. *The Handbook of Infrared and Raman Characteristic Frequencies of Organic Molecules*; Academic Press: New York, 1991.
(61) Mitsui, K.; Ukaji, T. Infrared Spectra of Some Aqueous Solutions. *Res. Rep. Ikutoku Tech. Univ.* **1977**, *B-2*, 77−82.
(62) Tarbuck, T. L.; Ota, S. T.; Richmond, G. L. Spectroscopic Studies of Solvated Hydrogen and Hydroxide Ions at Aqueous Surfaces. *J. Am. Chem. Soc.* **2006**, *128*, 14519−14527.
(63) Tyrode, E.; Johnson, C. M.; Kumpulainen, A.; Rutland, M. W.; Claesson, P. M. Hydration State of Nonionic Surfactant Monolayers at the Liquid/Vapor Interface: Structure Determination by Vibrational Sum Frequency Spectroscopy. *J. Am. Chem. Soc.* **2005**, *127*, 16848−16859.
(64) Rosen, M. J. *Surfactants and Interfacial Phenomena*, 3rd ed.; John Wiley & Sons: New York, 2004.
(65) Clegg, S. L.; Seinfeld, J. H. Thermodynamic Models of Aqueous Solutions Containing Inorganic Electrolytes and Dicarboxylic Acids at 298.15 K. 1. The Acids as Nondissociating Components. *J. Phys. Chem. A* **2006**, *110*, 5692−5717.
(66) Rao, Y.; Li, X.; Lei, X.; Jockusch, S.; George, M. W.; Turro, N. J.; Eisenthal, K. B. Observations of Interfacial Population and Organization of Surfactants with Sum Frequency Generation and Surface Tension. *J. Phys. Chem. C* **2001**, *115*, 12064−12067.
(67) *CRC Handbook of Chemistry and Physics*, 85th ed.; CRC Press: Boca Raton, FL, 2004.
(68) Lange, N. A. *Handbook of Chemistry*, Revised 10th ed.; McGraw-Hill: New York, 1967.
(69) Pool, R. E.; Versluis, J.; Backus, E. H. G.; Bonn, M. Comparative Study of Direct and Phase-Specific Vibrational Sum-Frequency Generation Spectroscopy: Advantages and Limitations. *J. Phys. Chem. B* **2011**, *115*, 15362−15369.
(70) Jena, K. C.; Covert, P. A.; Hall, S. A.; Hore, D. K. Absolute Orientation of Ester Side Chains on the PMMA surface. *J. Phys. Chem. C* **2011**, *115*, 15570−15574.

(71) Nguyen, T. H.; Hibbs, D. E.; Howard, S. T. Conformatioms, Energies, and Intramolecular Hydrogen Bonds in Dicarboxylic Acids: Implications of the Design of Synthetic Dicarboxylic Acid Receptors. *J. Comput. Chem.* **2005**, *26*, 1233−1241.
(72) Merchán, M.; Tomás, F.; Nebot-Gil, I. An ab initio study of intramolecular hydrogen bonding in malonic acid and its monoanion. *J. Mol. Struct. (THEOCHEM)* **1984**, *109*, 51−60.